Available online at www.sciencedirect.com

ScienceDirect

Applied Mathematical Modelling 31 (2007) 1444–1459

APPLIED MATHEMATICAL MODELLING

www.elsevier.com/locate/apm

Conduction and convection phenomena through a slab with thermal heterogeneities

A. Tadeu *, N. Simões

Department of Civil Engineering, Faculty of Sciences and Technology, University of Coimbra, Polo II, Pinhal de Marrocos, 3030-290 Coimbra, Portugal

Received 1 June 2005; received in revised form 1 November 2005; accepted 12 April 2006
Available online 30 June 2006

Abstract

This paper addresses the computation of the three-dimensional transient heat transfer through a layered solid and/or fluid formation containing irregular inclusions. The use of appropriate Green's functions for a flat layer formation in a boundary element method formulation avoids the discretization of the layer interface boundaries.

Both conduction and convection are taken into account in the heat diffusion generated by a source, placed somewhere in the layered system, assuming a known convection velocity field. This work is an extension of earlier work by the authors, in which only the conduction phenomenon was considered. As before, the calculation process is defined first in the frequency domain, while the final time series are later computed by applying inverse (fast) Fourier transforms. Once again, complex frequencies are used in order to avoid aliasing phenomena.

The applicability of the model is illustrated by solving the case of a solid layer submerged in a fluid medium and containing multiple circular cylindrical thermal heterogeneities. The importance of convection phenomena is studied for different inclusions' thermal properties.

Keywords: Transient heat transfer; Conduction; Convection; Boundary element method; 2.5D Green's functions; Frequency domain; Fourier transform

1. Introduction

Analytical solutions can only be used to solve simple problems, while the boundary element method (BEM) can be applied to deal with general problems. The BEM provides an alternative to the well established finite element method (FEM) for solving physical problems, such as that of heat diffusion, for which BEM codes have been developed by various authors, including Brebbia et al. [1], Pina and Fernandez [2]. Most of the known techniques that use BEM to solve transient heat transfer problems utilize "time marching schemes" or Laplace transforms.

* Corresponding author. Tel.: +351 239797204; fax: +351 239797190.
E-mail address: tadeu@dec.uc.pt (A. Tadeu).

0307-904X/$ - see front matter
doi:10.1016/j.apm.2006.04.010

As examples of "time marching" approaches, several works can be cited: Chang et al. [3] and Shaw [4] used a time-dependent fundamental solution for studying transient heat processes; later, Wrobel and Brebbia [5] described a formulation for axisymmetric diffusion problems; Carini et al. [6] implemented a symmetric boundary element method for studying the transient heat conduction over a two-dimensional homogeneous domain using semi-analytical integrations; also using a time marching boundary element method, Lesnic et al. [7] solved the unsteady diffusion equation in both one and two dimensions, taking into account the treatment of singularities.

As mentioned above, an alternative numerical scheme, the Laplace transform technique, can be implemented, too, to solve heat transfer problems. The purpose is to remove the time-dependent derivative, using instead a transform variable. However, this process then requires an inverse transform to find the solution in the time domain. A Laplace transform boundary element method approach was used, for example, by Sutradhar et al. [8,9] to solve the three-dimensional transient heat conduction in functionally graded materials.

Several numerical schemes have been proposed to improve the efficiency of the BEM and its applicability to more general problems, such as those involving nonlinearities. The dual reciprocity boundary method (DRBEM) is one of these techniques, and this was originally proposed by Nardini and Brebbia [10]. A number of works were subsequently published, including those by Satravaha and Zhu [11,12], applying the Laplace transform dual reciprocity method to the case of transient heat conduction in the presence of nonlinear material properties (thermal conductivity, density and specific heat coefficients were all assumed to be functions of temperature), boundary conditions and sources. Guven and Madenci [13] developed a coupled finite element–boundary element analysis method for the solution of transient two-dimensional heat conduction of domains with dissimilar materials and geometric discontinuities. Tanaka and Tanaka [14] studied the heat conduction in anisotropic non-homogeneous media using a BEM formulation based on the application of fundamental solutions for a fictitious homogeneous medium. This approach was first used by Butterfield for potential flow problems [15]. In order to study the transient heat conduction with nonlinear source terms in a domain where the thermal material properties change in spatial co-ordinates Sladek et al. [16] applied a local boundary integral equation method.

The BEM requires the discretization of the solid and fluid thermal interfaces and the knowledge of fundamental solutions. The definition of suitable Green's functions can avoid the discretization of some of those thermal interfaces, leading to a more efficient formulation. This paper computes the three-dimensional transient heat transfer through a flat-layered formation that contains heterogeneities, using Green's functions that avoid the discretization of the flat interfaces.

The technique proposed in this paper is an adaptation and extension of a formulation used by the authors to solve a similar problem, where only the conduction phenomenon was addressed [17]. In the work described here, both the conduction and the convection phenomena are taken into account with a pre-prescribed convection velocity.

The technique proposed makes use of time Fourier transforms to allow the calculations to be made in the frequency domain. This procedure overcomes some of the difficulties posed by the "time marching" and Laplace transforms approach, which may lead to loss of accuracy and the amplification of small truncation errors. If a spatial Fourier transform is then applied in the z and x directions the three-dimensional solution can be obtained as a sum of 2D problems with different spatial wavenumbers k_z and k_x.

The Green's functions for a layered medium, without heterogeneities, can be obtained as a superposition of heat plane sources, as was described originally by Lamb [18] for the propagation of elastodynamic waves in two-dimensional media. This approach was later adopted by other authors, such as Bouchon [19] and Tadeu and António [20] to compute three-dimensional elastodynamic fields using a discrete wave number representation. The solution can be expressed as the sum of the heat source terms equal to those in the unbounded space and the surface terms. These last terms need to satisfy the boundary conditions at the flat layer interfaces: continuity of normal fluxes and temperatures.

This paper first defines the three-dimensional problem and describes how the solution for a point source, applied in an infinite domain, can be written as a continuous superposition of heat plane terms, in the frequency domain. The time domain solutions, obtained after applying inverse frequency and spatial Fourier transforms, are compared with analytical solutions [21,22]. Next, the analytical Green's functions for a layer

formation bounded by two semi-infinite media are described, implemented and compared with those computed by the BEM model, which incorporates Green's functions for an unbounded medium and have the disadvantage of requiring the discretization of the boundary interfaces. Notice that the extension of the interfaces' discretization is limited by introducing damping; otherwise the system of equations involved would be too large to be solved.

These Green's functions are then incorporated into a BEM code to compute the heat transfer in the presence of cylindrical thermal heterogeneities placed in a solid layer bounded by two semi-infinite layers. Different simulations are performed to illustrate the applicability of the proposed model, and to evaluate the importance of the convection phenomena and the presence of thermal heterogeneities in heat diffusion across a solid layer bounded by fluid media.

2. 3D problem formulation

Transient heat transfer by conduction and convection in a homogeneous, isotropic body can be modelled by

$$\left(\frac{\partial^2}{\partial x^2}+\frac{\partial^2}{\partial y^2}+\frac{\partial^2}{\partial z^2}\right)T-\frac{1}{K}\left(V_x\frac{\partial}{\partial x}+V_y\frac{\partial}{\partial y}+V_z\frac{\partial}{\partial z}\right)T=\frac{1}{K}\frac{\partial T}{\partial t}, \tag{1}$$

in which V_x, V_y and V_z are the pre-prescribed velocity components in directions x, y and z respectively, t is time, $T(t,x,y,z)$ is temperature, $K=k/(\rho c)$ is the thermal diffusivity, k is the thermal conductivity, ρ is the density and c is the specific heat. A Fourier transformation in the time domain applied to Eq. (1) gives the equation below, expressed in the frequency domain

$$\left(\left(\frac{\partial^2}{\partial x^2}+\frac{\partial^2}{\partial y^2}+\frac{\partial^2}{\partial z^2}\right)-\frac{1}{K}\left(V_x\frac{\partial}{\partial x}+V_y\frac{\partial}{\partial y}+V_z\frac{\partial}{\partial z}\right)+\left(\sqrt{\frac{-\mathrm{i}\omega}{K}}\right)^2\right)\widehat{T}(\omega,x,y,z)=0, \tag{2}$$

where $\mathrm{i}=\sqrt{-1}$ and ω is the frequency. Eq. (2) differs from the Helmholtz equation by the presence of a convective term. For a heat point source, applied at $(0,0,0)$ in an unbounded medium, of the form $p(\omega,x,y,z,t)=\delta(x)\delta(y)\delta(z)\mathrm{e}^{\mathrm{i}(\omega t)}$, where $\delta(y)$ and $\delta(z)$ are Dirac-delta functions, the fundamental solution of Eq. (2) (see [22]) can be expressed as

$$\widehat{T}_f(\omega,x,y,z)=\frac{\mathrm{e}^{\frac{V_xx+V_yy+V_zz}{2K}}}{2k\sqrt{x^2+y^2+z^2}}\mathrm{e}^{-\mathrm{i}\sqrt{-\frac{V_x^2+V_y^2+V_z^2}{4K^2}-\frac{\mathrm{i}\omega}{K}}\sqrt{x^2+y^2+z^2}}. \tag{3}$$

To avoid the computational requirements of 3D problem formulation when the geometry of the problem remains constant along the z direction, the full 3D problem can be expressed as a summation of simpler 2D solutions. This requires the application of a Fourier transformation along that direction, writing this as a summation of 2D solutions with different spatial wavenumbers k_z (see [23]). The application of a spatial Fourier transformation to

$$\frac{\mathrm{e}^{-\mathrm{i}\sqrt{-\frac{V_x^2+V_y^2+V_z^2}{4K^2}-\frac{\mathrm{i}\omega}{K}}\sqrt{x^2+y^2+z^2}}}{\sqrt{x^2+y^2+z^2}}, \tag{4}$$

along the z direction, leads to this fundamental solution

$$\widetilde{T}_f(\omega,x,y,k_z)=\frac{-\mathrm{i}\mathrm{e}^{\frac{V_xx+V_yy+V_zz}{2K}}}{4k}\mathrm{H}_0\left(\sqrt{-\frac{V_x^2+V_y^2+V_z^2}{4K^2}-\frac{\mathrm{i}\omega}{K}-(k_z)^2}r_0\right), \tag{5}$$

where $\mathrm{H}_0(\,)$ are Hankel functions of the second kind and order 0, and $r_0=\sqrt{x^2+y^2}$.

This response is related to a spatially varying heat line source of the type $p(\omega,x,y,k_z,t)=\delta(x)\delta(y)\mathrm{e}^{\mathrm{i}(\omega t-k_zz)}$ (see Fig. 1).

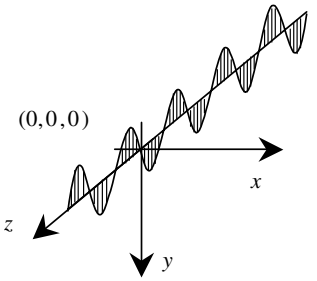

Fig. 1. Spatially harmonic varying line load.

The full three-dimensional solution can be synthesized by applying an inverse Fourier transform along the k_z domain to the expression $\frac{-\mathrm{i}}{2}\mathrm{H}_0\left(\sqrt{-\frac{V_x^2+V_y^2+V_z^2}{4K^2}-\frac{\mathrm{i}\omega}{K}-(k_z)^2}r_0\right)$,

$$\widetilde{T}(\omega,x,y,z)=\frac{\mathrm{e}^{\frac{V_x x+V_y y+V_z z}{2K}}}{2k\sqrt{x^2+y^2+z^2}}\int_{-\infty}^{\infty}\frac{-\mathrm{i}}{2}\mathrm{H}_0\left(\sqrt{-\frac{V_x^2+V_y^2+V_z^2}{4K^2}-\frac{\mathrm{i}\omega}{K}-(k_z)^2}r_0\right)\mathrm{e}^{-\mathrm{i}k_z z}\,\mathrm{d}k_z. \tag{6}$$

Assuming the existence of virtual sources, equally spaced at L_z, along z, then Eq. (6) changes into

$$\widetilde{T}(\omega,x,y,z)=\frac{\mathrm{e}^{\frac{V_x x+V_y y+V_z z}{2K}}}{2k\sqrt{x^2+y^2+z^2}}\int_{-\infty}^{\infty}\frac{-\mathrm{i}}{2}\mathrm{H}_0\left(\sqrt{-\frac{V_x^2+V_y^2+V_z^2}{4K^2}-\frac{\mathrm{i}\omega}{K}-(k_z)^2}r_0\right)\mathrm{e}^{-\mathrm{i}k_z z}\sum_{m=-\infty}^{\infty}\mathrm{e}^{-\mathrm{i}k_{zm}L_z}\,\mathrm{d}k_z. \tag{7}$$

Using the results from distribution theory (e.g. [24]) this equation can be expressed as

$$\widetilde{T}(\omega,x,y,z)=\frac{2\pi}{L_z}\frac{\mathrm{e}^{\frac{V_x x+V_y y+V_z z}{2K}}}{2k\sqrt{x^2+y^2+z^2}}\sum_{m=-\infty}^{\infty}\mathrm{H}_0\left(\sqrt{-\frac{V_x^2+V_y^2+V_z^2}{4K^2}-\frac{\mathrm{i}\omega}{K}-(k_{zm})^2}r_0\right)\mathrm{e}^{-\mathrm{i}k_{zm}z}, \tag{8}$$

where k_{zm} is the axial wavenumber given by $k_{zm}=\frac{2\pi}{L_z}m$. Eq. (8) can be approximated in turn by a finite discrete summation, which enables the solution to be obtained by solving a limited number of two-dimensional problems,

$$\widetilde{T}(\omega,x,y,z)=\frac{2\pi}{L_z}\frac{\mathrm{e}^{\frac{V_x x+V_y y+V_z z}{2K}}}{2k\sqrt{x^2+y^2+z^2}}\sum_{m=-M}^{M}\mathrm{H}_0\left(\sqrt{-\frac{V_x^2+V_y^2+V_z^2}{4K^2}-\frac{\mathrm{i}\omega}{K}-(k_{zm})^2}r_0\right)\mathrm{e}^{-\mathrm{i}k_{zm}z}. \tag{9}$$

The distance L_z must be large enough to prevent spatial contamination from the virtual sources [25]. An analogous approach has been used by Tadeu et al. [26] and Godinho et al. [27] to solve problems of wave propagation.

The fundamental solution of the differential equation obtained from Eq. (2) after the application of a spatial Fourier transformation along the z direction (see Eq. (10)) is Eq. (5), with $V_z=0$.

$$\left(\left(\frac{\partial^2}{\partial x^2}+\frac{\partial^2}{\partial y^2}\right)-\frac{1}{K}\left(V_x\frac{\partial}{\partial x}+V_y\frac{\partial}{\partial y}\right)+\left(\sqrt{\frac{-\mathrm{i}\omega}{K}-(k_z)^2}\right)^2\right)\widetilde{T}(\omega,x,y,k_z)=0. \tag{10}$$

Eq. (5), for a spatially sinusoidal harmonic heat line source applied at the point (0,0) along the z direction, subject to convection velocities V_x, V_y and V_z, can be further manipulated and written as a continuous superposition of heat plane phenomena, as in Garvin [28],

$$\widetilde{T}_f(\omega,x,y,k_z)=\frac{-\mathrm{i}\mathrm{e}^{\frac{V_x x+V_y y+V_z z}{2K}}}{4\pi k}\int_{-\infty}^{+\infty}\left(\frac{\mathrm{e}^{-\mathrm{i}\nu|y|}}{\nu}\right)\mathrm{e}^{-\mathrm{i}k_x(x)}\,\mathrm{d}k_x, \tag{11}$$

where $v = \sqrt{-\frac{V_x^2+V_y^2+V_z^2}{2K} - \frac{i\omega}{K} - (k_z)^2 - k_x^2}$ with $(\mathrm{Im}(v) \leqslant 0)$, and the integration is related to the horizontal wave number (k_x) along the x direction. The use of the expansion of the Hankel function is described by Morse and Feshbach [29].

Assuming the existence of an infinite number of virtual sources, these continuous integrals can be transformed into a summation if an infinite number of such sources is distributed along the x direction, spaced at equal intervals L_x. The above equation can then be written as

$$\widetilde{T}_f(\omega,x,y,k_z) = \frac{-ie^{\frac{V_x x+V_y y+V_z z}{2K}}}{4k} E_0 \sum_{n=-\infty}^{n=+\infty} \left(\frac{E}{v_n}\right) E_d, \tag{12}$$

where $E_0 = \frac{-i}{2kL_x}$, $E = e^{-iv_n|y|}$, $E_d = e^{-ik_{xn}(x)}$, $v_n = \sqrt{-\frac{V_x^2+V_y^2+V_z^2}{4K^2} - \frac{i\omega}{K} - (k_z)^2 - k_{xn}^2}$ with $(\mathrm{Im}(v_n) \leqslant 0)$, $k_{xn} = \frac{2\pi}{L_x} n$, which can in turn be approximated by a finite sum of equations (N). Note that $k_z = 0$ corresponds to the two-dimensional case.

2.1. Responses in the time domain

The heat responses in the spatial–temporal domain are obtained by means of an inverse fast Fourier transform in k_z and k_x and in the frequency domain. In order to prevent the aliasing phenomena, complex frequencies with a small imaginary part of the form $\omega_c = \omega - i\eta$ (with $\eta = 0.7\Delta\omega$, and $\Delta\omega$ being the frequency step) are used in the computation procedure. The constant η cannot be made arbitrarily large, since this leads either to severe loss of numerical precision, or to underflows and overflows in the evaluation of the exponential windows (see [30]). The time evolution of the heat source amplitude can be diversified. The time Fourier transformation of the incident heat field defines the frequency domain where the BEM solution needs to be computed. The response may need to be computed from 0.0 Hz up to very high frequencies. An intrinsic characteristic of this problem is that the heat responses decay very fast as the frequency increases, which allows us to limit the upper frequency for the solution. The static response can be computed when the frequency is zero, since the use of complex frequencies leads to arguments for the Hankel function that are different from zero ($\omega_c = -i\eta$ for 0.0 Hz).

2.2. Verification of the solution

The formulation described above was verified by computing heat propagation in an unbounded medium when conduction and convection are considered. The results obtained were compared with the analytical response in the time domain.

The exact solution of the three, two or one-dimensional convective diffusion, expressed by Eq. (1), in an unbounded medium subjected to a unit heat source can be found in the literature, see Banerjee [21]. The time solution at (x,y,z) for a unit heat source placed at $(0,0,0)$ at time $t = t_0$ in an unbounded medium is given by the expression

$$T(t,x,y,z) = \frac{e^{\frac{-(-\tau V_x+x)^2-(-\tau V_y+y)^2-(-\tau V_z+z)^2}{4K\tau}}}{\rho c(4\pi K\tau)^{d/2}}, \quad \text{if } t > t_0, \tag{13}$$

where $\tau = t - t_0$; the parameter d can be 3, 2 or 1 depending on whether we are in the presence of a three, two or one-dimensional problem, respectively.

The verification example assumes that a homogeneous unbounded medium was excited by a cylindrical heat source ($d = 2$) placed at $(0,0,0)$. The material's density (ρ), specific heat (c), and the thermal conductivity (k) attributed to the medium were 2300 kg m^{-3}, 880.0 J kg^{-1} °C^{-1} and 1.4 W m^{-1} °C^{-1}, respectively. The convection velocity ascribed in the x, y directions was 1×10^{-6} m/s.

The heat responses were calculated along a line of 40 receivers placed from $(x = -1.5,\ y = 0.35,\ z = 0)$ to $(x = 1.5,\ y = 0.35,\ z = 0)$. The calculations, using the formulation described above, were done in the frequency range $[0, 1024 \times 10^{-7}\ \mathrm{Hz}]$ with an increment of $\Delta\omega = 10^{-7}$ Hz, which defines a time window of $T = 2777.8$ h.

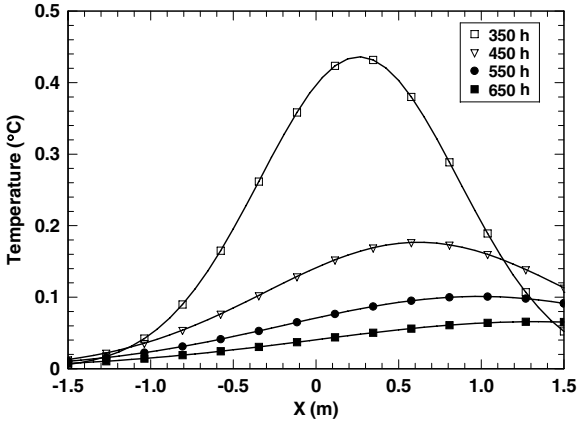

Fig. 2. Temperature distribution along a line of 40 receivers, at different times (350 h, 450 h, 550 h and 650 h) for a cylindrical ($d = 2$) unit heat source.

The correspondent time domain responses were obtained by applying a numerical inverse fast Fourier transform in k_z and in the frequency domain. These responses are illustrated in Fig. 2 by marks, while the solid lines indicate the solution computed using Eq. (13). The two solutions show good agreement. It is interesting to note that the response is not symmetric because of the convection phenomenon in the x direction.

2.3. 2.5D heat diffusion Green's functions in a flat layer bounded by two unbounded media

The Green's functions for a system composed of a layer placed between two semi-infinite media (see Fig. 3), with known vertical convection velocity, can be established by imposing the required boundary conditions at the interfaces, which are in this case the continuity of temperatures and heat fluxes. So, the heat will flow from the source position layer through the interfaces to the other media. The conduction and convection phenomena in this propagation process can be modelled. This process assumes that there is an inflowing mass along the boundary that verifies the mass conservation.

The definition of the solution involves two different kinds of terms: the source terms and the surface terms. The source terms, which can also be designated as the incident field, are equal to those in the full-space, while the surface terms need to satisfy the continuity of temperatures and normal fluxes at the interfaces. These two terms can be expressed in a similar form. For a heat source located at (x_0, y_0, z_0), the terms generated in either side of the interfaces (see Fig. 3) are expressed as follows:

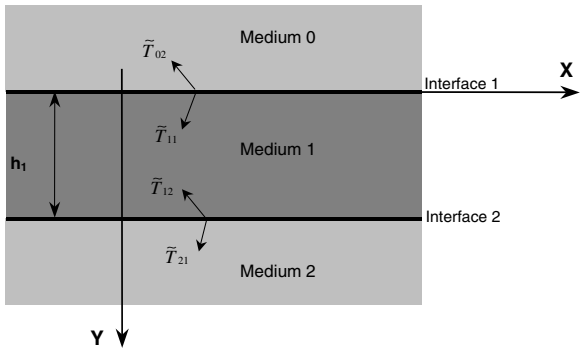

Fig. 3. Geometry of the problem for a flat solid or fluid layer bounded by two semi-infinite solid or fluid media.

Upper semi-infinite space (*interface 1*)

$$\widetilde{T}_{02}(\omega,x,y,k_z) = E_{00}\mathrm{e}^{\frac{V_{y0}(y-y_0)}{2K_0}}\sum_{n=-\infty}^{n=+\infty}\left(\frac{E_{01}}{v_{n0}}A^b_{n0}\right)E_{\mathrm{d}}; \tag{14}$$

Solid layer (*interface 1*)

$$\widetilde{T}_{11}(\omega,x,y,k_z) = E_{01}\mathrm{e}^{\frac{V_{y1}(y-y_0)}{2K_1}}\sum_{n=-\infty}^{n=+\infty}\left(\frac{E_{11}}{v_{n1}}A^t_{n1}\right)E_{\mathrm{d}}; \tag{15}$$

Solid layer (*interface 2*)

$$\widetilde{T}_{12}(\omega,x,y,k_z) = E_{01}\mathrm{e}^{\frac{V_{y1}(y-y_0)}{2K_1}}\sum_{n=-\infty}^{n=+\infty}\left(\frac{E_{12}}{v_{n1}}A^b_{n1}\right)E_{\mathrm{d}}; \tag{16}$$

Lower semi-infinite space (*interface 2*)

$$\widetilde{T}_{21}(\omega,x,y,k_z) = E_{02}\mathrm{e}^{\frac{V_{y2}(y-y_0)}{2K_2}}\sum_{n=-\infty}^{n=+\infty}\left(\frac{E_{21}}{v_{n2}}A^t_{n2}\right)E_{\mathrm{d}}, \tag{17}$$

where $E_{0j} = -\mathrm{i}/2k_jL_x$, $E_{00} = \mathrm{e}^{-\mathrm{i}v_{n0}y}$, $E_{11} = \mathrm{e}^{-\mathrm{i}v_{n1}y}$, $E_{12} = \mathrm{e}^{-\mathrm{i}v_{n1}|y-h_1|}$, $E_{21} = \mathrm{e}^{-\mathrm{i}v_{n2}|y-h_1|}$ and $v_{nj} = \sqrt{-(V_{yj}/2K_j)^2 - \mathrm{i}\omega/K_j - k_z^2 - k_{xn}^2}$ with $\mathrm{Im}(v_{nj}) \leqslant 0$ ($j = 1$ corresponds to the intermediate layer (medium 1), while $j = 0$ and $j = 2$ indicate the upper and lower semi-infinite media, respectively (medium 0, 2)). Meanwhile, $K_j = k_j/\rho_j c_j$ is the thermal diffusivity in the medium j (k_j, ρ_j and c_j are the thermal conductivity, the density and the specific heat of the material in the medium, j, respectively) and V_{yj} is the convection in the y direction in the fluid medium j.

The unknown coefficients A^b_{n0}, A^t_{n1}, A^b_{n1} and A^t_{n2} are computed by establishing the appropriate boundary conditions, so that the field produced simultaneously by the source and surface terms leads to the continuity of heat fluxes and temperatures at $y = h_1$ and $y = 0$. Assuming that the heat source is in the intermediate layer, the following system results when the boundary conditions are imposed for each value of n:

$$\begin{bmatrix} \left[\frac{V_{y0}}{2K_0} + \mathrm{i}v_{n0}\right]\frac{c_{10}}{c_{21}} & -\left[\frac{V_{y1}}{2K_1} - \mathrm{i}v_{n1}\right] & -\left[\frac{V_{y1}}{2K_1} + \mathrm{i}v_{n1}\right]\mathrm{e}^{-\mathrm{i}v_{n1}h_1} & 0 \\ \frac{k_1c_{30}}{k_0c_{41}} & -1 & -\mathrm{e}^{-\mathrm{i}v_{n1}h_1} & 0 \\ 0 & \left[\frac{V_{y1}}{2K_1} - \mathrm{i}v_{n1}\right]\mathrm{e}^{-\mathrm{i}v_{n1}h_1} & \left[\frac{V_{y1}}{2K_1} + \mathrm{i}v_{n1}\right] & -\left[\frac{V_{y2}}{2K_2} - \mathrm{i}v_{n2}\right]\frac{c_{22}}{c_{11}} \\ 0 & \mathrm{e}^{-\mathrm{i}v_{n1}h_1} & 1 & -\frac{k_1c_{22}}{k_2c_{11}} \end{bmatrix} \begin{bmatrix} A^b_{n0} \\ A^t_{n1} \\ A^b_{n1} \\ A^t_{n2} \end{bmatrix} = \begin{bmatrix} b_1 \\ b_2 \\ b_3 \\ b_4 \end{bmatrix}, \tag{18}$$

where $c_{1j} = \frac{1}{v_{nj}}\mathrm{e}^{\frac{V_{yj}(\sum_{l=1}^{j}h_l - y_0)}{2K_j}}$, $c_{2j} = \frac{1}{v_{nj}}\mathrm{e}^{\frac{V_{yj}(\sum_{l=1}^{j-1}h_l - y_0)}{2K_j}}$, while $b_1 = [V_{y1}/2K_1 + \mathrm{i}v_{n1}]\mathrm{e}^{-\mathrm{i}v_{n1}y_0}$, $b_2 = \mathrm{e}^{-\mathrm{i}v_{n1}y_0}$, $b_3 = -[V_{y1}/2K_1 - \mathrm{i}v_{n1}]\mathrm{e}^{-\mathrm{i}v_{n1}|h_1-y_0|}$ and $b_4 = -\mathrm{e}^{-\mathrm{i}v_{n1}|h_1-y_0|}$, if the source is in the intermediate layer ($0 < y_0 < h_1$).

The temperature for the three-layer media is computed by adding the contribution of the source terms to that associated with the surface terms originated at the various interfaces. This leads to the following expressions for the temperatures in the three media, when the source is in the intermediate layer,

$$\begin{aligned} \widetilde{T}(\omega,x,y,k_z) &= E_{00}\mathrm{e}^{\frac{V_{y0}(y-y_0)}{2K_0}}\sum_{n=-\infty}^{n=+\infty}\left(\frac{E_{01}}{v_{n0}}A^b_{n0}\right)E_{\mathrm{d}}, \quad \text{if } y < 0, \\ \widetilde{T}(\omega,x,y,k_z) &= \frac{-\mathrm{i}}{4k_1}\mathrm{e}^{\frac{V_{y1}(y-y_0)}{2K_1}}\mathrm{H}_0(K_{t1}r_1) + E_{01}\mathrm{e}^{\frac{V_{y1}(y-y_0)}{2K_1}} \\ &\quad \times \sum_{n=-\infty}^{n=+\infty}\left(\frac{E_{11}}{v_{n1}}A^t_{n1} + \frac{E_{12}}{v_{n1}}A^b_{n1}\right)E_{\mathrm{d}}, \quad \text{if } 0 < y < h_1, \\ \widetilde{T}(\omega,x,y,k_z) &= E_{02}\mathrm{e}^{\frac{V_{y2}(y-y_0)}{2K_2}}\sum_{n=-\infty}^{n=+\infty}\left(\frac{E_{21}}{v_{n2}}A^t_{n2}\right)E_{\mathrm{d}}, \quad \text{if } y > h_1, \end{aligned} \tag{19}$$

where $K_{t1} = \sqrt{-\frac{V_{y1}^2}{4K_1^2} - \frac{\mathrm{i}\omega}{K_1} - (k_z)^2}$ and $r_1 = \sqrt{(x-x_0)^2 + (y-y_0)^2}$.

This derivation assumes that the spatially sinusoidal harmonic heat source is located in the intermediate layer. However, the equations can be easily manipulated to cater for another position of the source.

3. Boundary element formulation

The fundamental BEM equations are not described in detail here, since they can be found in Wrobel [5]. The boundary integral equations for a homogeneous isotropic medium layer that is embedded by an infinite medium and contains a cylindrical body (bounded by a surface S), when this system is subjected to an incident heat field given by $\widetilde{T}^{\text{inc}}$, are expressed as follows:

along the exterior domain

$$\begin{aligned}\overline{p}\widetilde{T}^{(\text{ext})}(x_0,y_0,k_z,\omega) = &\int_S q^{(\text{ext})}(x,y,\eta_n,k_z,\omega)G^{(\text{ext})}(x,y,x_0,y_0,k_z,\omega)\,\mathrm{d}s\\ &-\int_S H^{(\text{ext})}(x,y,\eta_n,x_0,y_0,k_z,\omega)\widetilde{T}^{(\text{ext})}(x,y,k_z,\omega)\,\mathrm{d}s\\ &-\int_S G^{(\text{ext})}(x,y,x_0,y_0,k_z,\omega)\widetilde{T}^{(\text{ext})}(x,y,k_z,\omega)V_n^{(\text{ext})}\,\mathrm{d}s+\widetilde{T}_{\text{inc}}(x_0,y_0,k_z,\omega),\end{aligned} \tag{20}$$

along the interior domain

$$\begin{aligned}\overline{p}\widetilde{T}^{(\text{int})}(x_0,y_0,k_z,\omega) = &\int_S q^{(\text{int})}(x,y,\eta_n,k_z,\omega)G^{(\text{int})}(x,y,x_0,y_0,k_z,\omega)\,\mathrm{d}s\\ &-\int_S H^{(\text{int})}(x,y,\eta_n,x_0,y_0,k_z,\omega)\widetilde{T}^{(\text{int})}(x,y,k_z,\omega)\,\mathrm{d}s\\ &-\int_S G^{(\text{int})}(x,y,x_0,y_0,k_z,\omega)\widetilde{T}^{(\text{int})}(x,y,k_z,\omega)V_n^{(\text{int})}\,\mathrm{d}s.\end{aligned} \tag{21}$$

The boundary integral equations incorporate a convective term, where $V_n = V_x n_x + V_y n_y$. In these equations, the superscripts "int" and "ext" refer to the interior and exterior domains respectively, η_n is the unit outward normal along the boundary, G and H are respectively the fundamental solutions (Green's functions) for the temperature ($\widetilde{T}$) and heat flux (q), at (x,y) due to a virtual point heat load at (x_0,y_0). The factor $\overline{p}$ is a constant defined by the shape of the boundary, taking the value 1/2 if the shape is smooth and $(x_0,y_0)\in S$. Note that this formulation assumes initial conditions of null temperatures and null heat fluxes throughout the domain. Other initial conditions would require the evaluation of surface or volume integrals.

If the boundary is discretized into N straight boundary elements, with one nodal point in the middle of each element, Eqs. (20) and (21) take the form:

along the exterior domain

$$\sum_{l=1}^{N} q^{(\text{ext})kl}G^{(\text{ext})kl} - \sum_{l=1}^{N}\widetilde{T}^{(\text{ext})kl}H^{(\text{ext})kl} - \sum_{l=1}^{N} G^{(\text{ext})kl}\widetilde{T}^{(\text{ext})kl}V_n^{(\text{ext})} + \widetilde{T}^{k}_{\text{inc}_l} = p_{kl}\widetilde{T}^{(\text{ext})kl}, \tag{22}$$

along the interior domain

$$\sum_{l=1}^{N} q^{(\text{int})kl}G^{(\text{int})kl} - \sum_{l=1}^{N}\widetilde{T}^{(\text{int})kl}H^{(\text{int})kl} - \sum_{l=1}^{N} G^{(\text{int})kl}\widetilde{T}^{(\text{int})kl}Vn^{(\text{int})} = p_{kl}\widetilde{T}^{(\text{int})kl}, \tag{23}$$

where

$q^{(\text{ext})kl}$ and $\widetilde{T}^{(\text{ext})kl}$ are the nodal heat fluxes and temperatures in the exterior domain,
$q^{(\text{int})kl}$ and $\widetilde{T}^{(\text{int})kl}$ are the nodal heat fluxes and temperatures in the interior domain,
$H^{(\text{ext})kl} = \int_{C_l} H^{(\text{ext})}(\omega,x_l,y_l,\eta_l,x_k,y_k,k_z)\,\mathrm{d}C_l$, $\quad H^{(\text{int})kl} = \int_{C_l} H^{(\text{int})}(\omega,x_l,y_l,\eta_l,x_k,y_k,k_z)\mathrm{d}C_l$,
$G^{(\text{ext})kl} = \int_{C_l} G^{(\text{ext})}(\omega,x_l,y_l,x_k,y_k,k_z)\,\mathrm{d}C_l$, $\quad G^{(\text{int})kl} = \int_{C_l} G^{(\text{int})}(\omega,x_l,y_l,x_k,y_k,k_z)\,\mathrm{d}C_l$,

where η_l is the unit outward normal for the lth boundary segment C_l. In Eqs. (22) and (23), $H^{(\mathrm{ext})}(\omega, x_l, y_l, \eta_l, x_k, y_k, k_z)$ and $G^{(\mathrm{ext})}(\omega, x_l, y_l, x_k, y_k, k_z)$ are respectively the Green's functions for the heat fluxes and temperature components in the exterior medium of the inclusion, that is, for a flat layer bounded by two unbounded media. $H^{(\mathrm{int})}(\omega, x_l, y_l, \eta_l, x_k, y_k, k_z)$ and $G^{(\mathrm{int})}(\omega, x_l, y_l, x_k, y_k, k_z)$ are respectively the Green's functions for the heat fluxes and temperature components in the interior medium of the inclusion, that is, for an unbounded medium, at point (x_l, y_l), caused by a concentrated heat load acting at the source point (x_k, y_k). If the loaded element coincides with the element being integrated, the factor p_{kl} takes the value 1/2.

The two-and-a-half dimensional Green's functions for temperature and heat fluxes in Cartesian co-ordinates are those for an unbounded medium,

$$\begin{aligned} G(x,y,x_0,y_0,k_z,\omega) &= \frac{-\mathrm{i}}{4k}\mathrm{e}^{\frac{Vr_0}{2K}}\mathrm{H}_0(k_{tr}r), \\ H(\omega,x_l,y_l,\eta_l,x_k,y_k,k_z) &= \frac{-\mathrm{i}}{4}\mathrm{e}^{\frac{Vr_0}{2K}}\left[\frac{V}{2K}\left(\frac{\partial r_0}{\partial \eta_l}\right)\mathrm{H}_0(k_{tr}r) - k_{tr}H_1(k_{tr}r)\left(\frac{\partial r}{\partial \eta_l}\right)\right], \end{aligned} \tag{24}$$

where V is the assumed radial convection velocity, $k_{tr} = \sqrt{\frac{-V^2}{4K^2} + \frac{-\mathrm{i}\omega}{K} - (k_z)^2}$, $r = \sqrt{(x_l - x_k)^2 + (y_l - y_k)^2}$, $r_0 = \sqrt{x^2 + y^2}$ is the distance to the convection source position, and $\mathrm{H}_n(\,)$ are Hankel functions of the second kind and order n.

If the element to be integrated is not the loaded element, the integrations in Eqs. (22) and (23) are evaluated using a Gaussian quadrature scheme, while for the loaded element, the existing singular integrands in the source terms of the Green's functions are calculated in closed form (see Tadeu et al. [31,32]).

The final system of equations is assembled assuring the continuity of temperatures and heat fluxes along the boundary of the inclusion. The unknown nodal temperatures and heat fluxes are obtained by solving this system of equations, allowing the heat field along the domain to be defined.

The final integral equations are manipulated and combined so as to impose the continuity of temperatures and heat fluxes along the boundary of the inclusion, and a system of equations is assembled. The solution of this system of equations gives the nodal temperatures and heat fluxes, which allow the reflected heat field to be defined.

4. Verification of the Green's functions

In order to verify the accuracy of the Green's functions, the results were compared with those arrived by applying the BEM model using the Green's solutions for an unbounded medium. BEM applications imply the discretization of all material interfaces. Notice that the BEM code implemented and used here was first tested using a simple problem geometry (circular cylindrical geometries), for which analytical solutions are known (not included here).

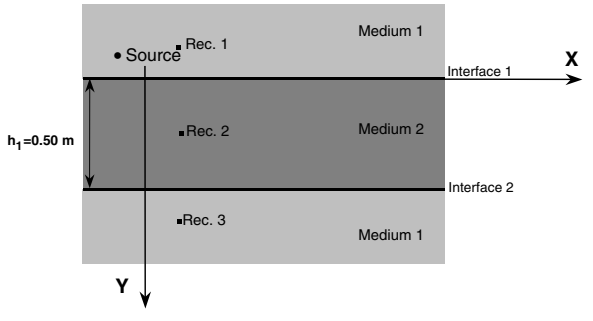

Fig. 4. Geometry of the problem used in the verification of the Green's functions. A 0.5 m thick layer (medium 2), bounded by two semi-infinite media (media 1).

Table 1
Material's thermal properties used for the verification of the Green's functions

	Medium 1	Medium 2
Thermal conductivity, k [W m^{-1} °C^{-1}]	0.72	1.4
Density, ρ [kg m^{-3}]	1860.0	2300.0
Specific heat, c_p [J kg^{-1} °C^{-1}]	780.0	880.0

The performance of the analytical Green's functions is illustrated using a system built by a layer (medium 2), 0.5 m thick, placed between two unbounded media (media 1), as shown in Fig. 4. A harmonic heat line source is applied in medium 2 at point ($x = -0.1$ m, $y = -0.1$ m). The thermal material properties of the layered formation are listed in Table 1. The convection velocities chosen for medium 1 and 2 were -1×10^{-7} m/s and 5×10^{-7} m/s, respectively.

Since complex frequencies are used, the full discretization of the layer interfaces is avoided, as described by Bouchon and Aki [25] and Phinney [33]. The distance that has been imposed for the discretization is given by the expression, $L_{\text{dist}} = 2\sqrt{k_j/(\rho_j c_j \Delta f)}$. In order to get the largest spatial distance, the thermal material properties used were those of medium 2, which allow the highest thermal diffusivity.

The computations were performed in the frequency range (0, $32 \times 0.5 \times 10^{-5}$ Hz), with a frequency increment of $\Delta\omega = 0.5 \times 10^{-5}$ Hz. Fig. 5 shows the real and imaginary parts of the heat responses at receivers Rec. 1 ($x = 0.1$ m, $y = -0.15$ m), Rec. 2 ($x = 0.1$ m, $y = 0.25$ m) and Rec. 3 ($x = 0.1$ m, $y = 0.65$ m) when $k_z = 0.4$ rad/m. The analytical responses are displayed by the solid lines, while the marks correspond to the BEM solution. The square and round marks correspond to the real and imaginary parts of the responses, respectively. The BEM model uses 200 constant boundary elements to discretize the layer interfaces.

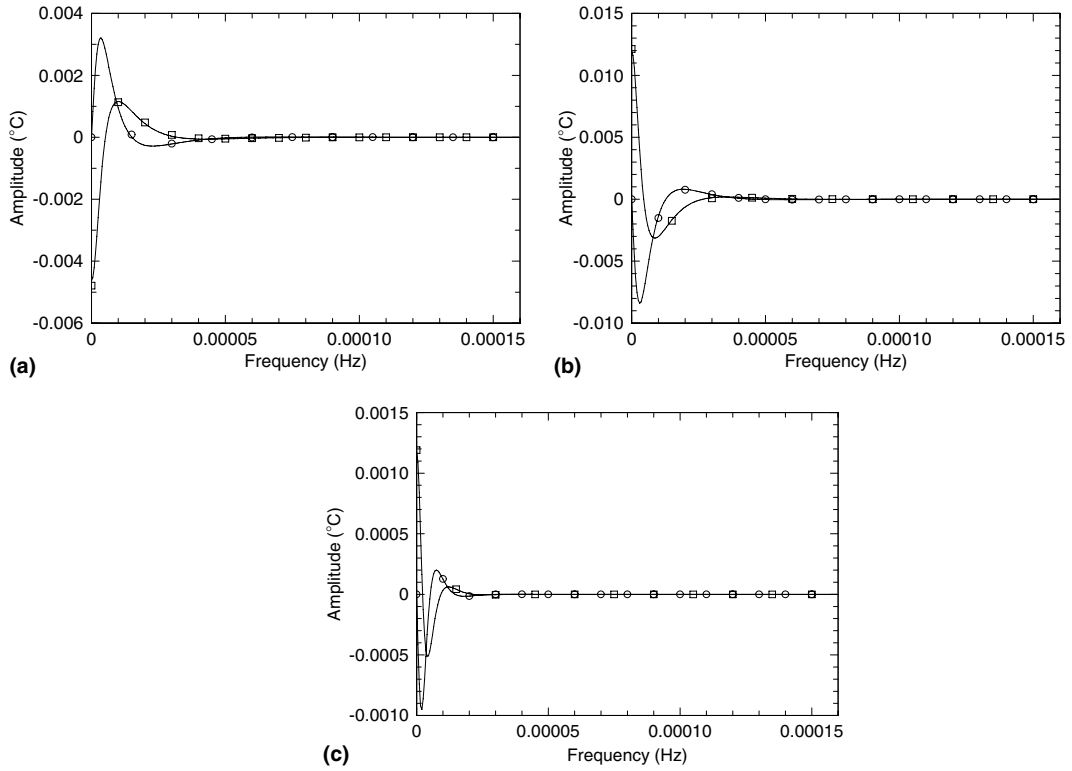

Fig. 5. Validation for a layer without inclusions bounded by two semi-infinite media. Frequency responses (real and imaginary parts): (a) Receiver Rec. 1; (b) Receiver Rec. 2; (c) Receiver Rec. 3.

These two solutions are in very close agreement. Equally good results were obtained from tests in which receivers and sources were placed at different points.

5. Verification of the BEM model using the proposed Green's functions

The BEM formulation using the Green's functions for a layered formation is implemented to compute the three-dimensional heat field generated by a spatially sinusoidal harmonic heat line source placed in a two-dimensional horizontal layer, 0.5 m thick, submerged in an unbounded fluid medium. This solid layer contains a circular cylindrical inclusion with radius 0.1 m and placed parallel to the solid layer interfaces (along the z

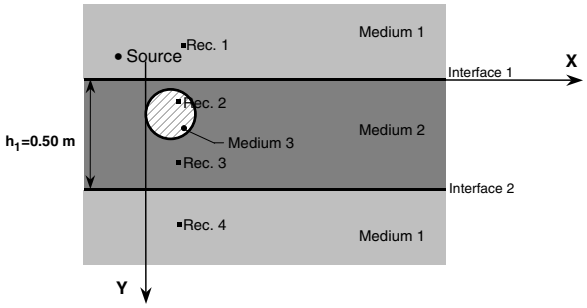

Fig. 6. Geometry of the problem for a layer (0.5 m thick) with a cylindrical circular inclusion (0.1 m radius), bounded by two semi-infinite media. Position of the heat source and of the receivers Rec. 1–4.

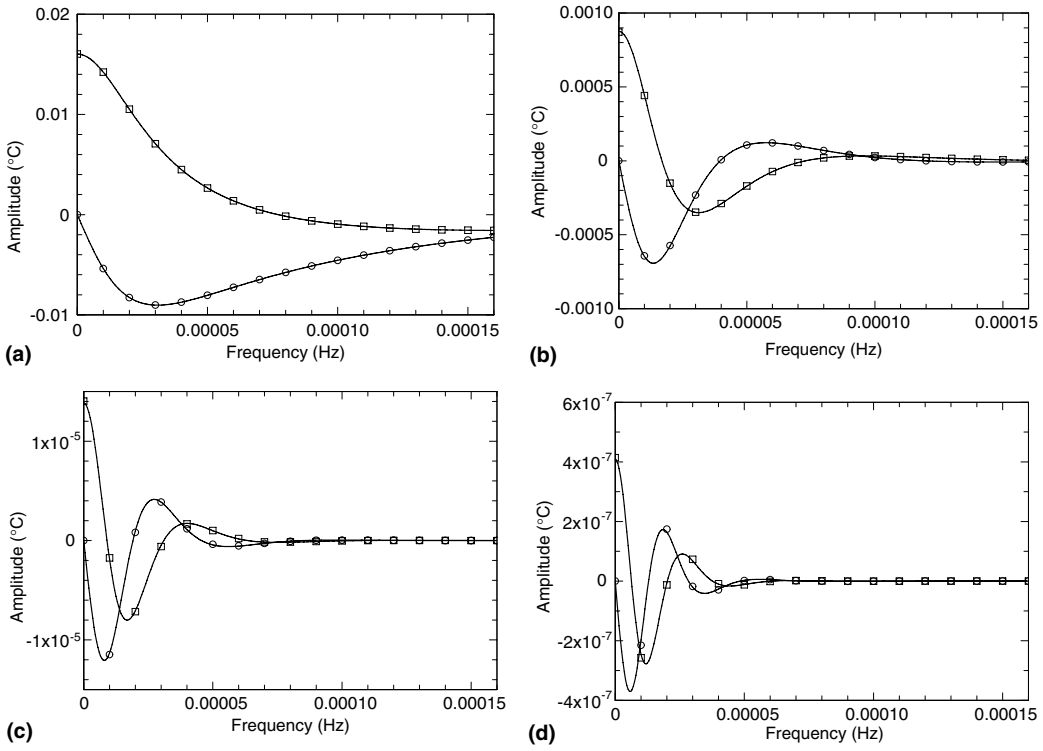

Fig. 7. Verification of the proposed BEM model applied to the case of a solid layer containing an inclusion bounded by two semi-infinite fluid media. Frequency responses at: (a) Receiver Rec. 1; (b) Receiver Rec. 2; (c) Receiver Rec. 3; (d) Receiver Rec. 4.

direction) (see Fig. 6). Incorporating the Green's functions, derived above, into the BEM formulation, the discretization is limited to the inclusion surface. The solutions obtained are compared with those given by the BEM formulation which uses the Green's functions only for the unbounded media and requires the additional discretization of the flat interfaces.

The properties and the assumed convection velocities of media 1 and 2 are the same as those used in verification section above, while the thermal properties and the convection velocity in the inclusion are assumed to be $k_3 = 0.12\ \mathrm{W\,m^{-1}\,°C^{-1}}$, $c_3 = 1380.0\ \mathrm{J\,kg^{-1}\,°C^{-1}}$ and $\rho_3 = 510\ \mathrm{kg\,m^{-3}}$ and -2×10^{-7} m/s, respectively. This system is heated by a harmonic line source located at ($x = -0.1$ m, $y = -0.1$ m). All the calculations are also performed in the frequency range $[0, 32\times0.5\times10^{-5}\ \mathrm{Hz}]$ with a frequency increment of $\Delta\omega = 10^{-5}$ Hz including a complex component given by η ($\eta = 0.7\Delta\omega$). Fig. 7 displays the real and imaginary parts of the responses at receivers 1–4 when $k_z = 0.4$ rad/m. The receivers Rec. 1–4 are placed at ($x = 0.1$ m, $y = -0.15$ m), ($x = 0.1$ m, $y = 0.1$ m), ($x = 0.1$ m, $y = 0.35$ m) and ($x = 0.1$ m, $y = 0.6$ m), respectively.

The solid lines represent responses of the proposed formulation, while the marks correspond to the BEM solutions using the full boundary discretization. The square and round marks indicate the real and imaginary parts of the BEM responses, respectively. The standard BEM uses 250 constant boundary elements to model the layer interfaces and the inclusion boundary, while the proposed model uses only 50 constant boundary elements to discretize the inclusion. All the plots reveal an excellent agreement between the two solutions presented.

6. Applications

In order to illustrate the applicability of the formulation presented above, several simulations have been performed. They use a layered system built with a solid concrete layer (medium 2) containing three inclusions (medium 3), and buried in two semi-infinite water media (medium 1). Inside the solid layer, 0.3 m thick, three cylindrical circular inclusions with 0.055 m of radius are modelled, as shown in Fig. 8a. The semi-infinite water media were assumed to allow both conduction and convection phenomena, while only the conduction phenomenon exists in the solid layer. This process assumes that there is an inflowing mass along the top of the upper and the bottom of the lower boundaries that verifies the mass conservation.

Two different systems are modelled: in the first (Case 1) the inclusions are made of polystyrene (with thermal properties $k = 0.027\ \mathrm{W\,m^{-1}\,°C^{-1}}$, $c = 1210\ \mathrm{J\,kg^{-1}\,°C^{-1}}$ and $\rho = 55\ \mathrm{kg\,m^{-3}}$); in the second (Case 2) steel properties (with thermal properties $k = 63.9\ \mathrm{W\,m^{-1}\,°C^{-1}}$, $c = 434.0\ \mathrm{J\,kg^{-1}\,°C^{-1}}$ and $\rho = 7832.0\ \mathrm{kg\,m^{-3}}$) were prescribed for the inclusions. The vertical convection velocities allowed at the top and bottom water medium were 2×10^{-6} m/s and 1×10^{-6} m/s, respectively.

The thermal conductivity, specific heat and density of the concrete layer are $k = 1.4\ \mathrm{W\,m^{-1}\,°C^{-1}}$, $c = 880\ \mathrm{J\,kg^{-1}\,°C^{-1}}$ and $\rho = 2300\ \mathrm{kg\,m^{-3}}$, respectively. The thermal properties of the top and bottom

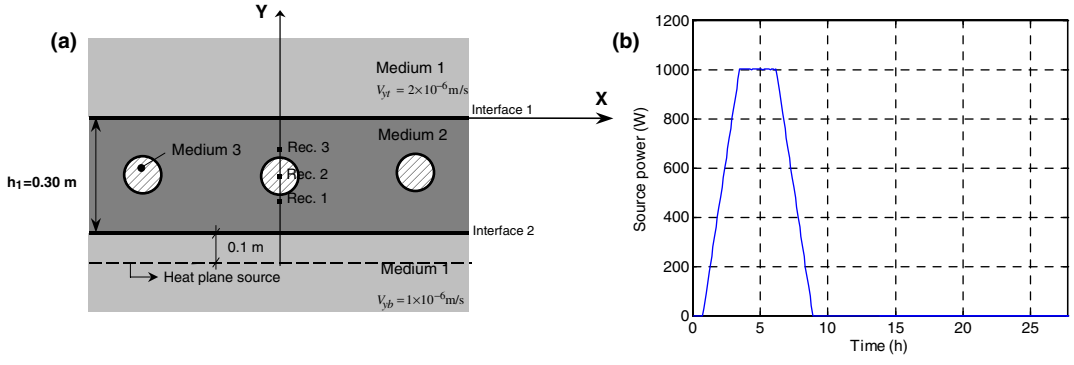

Fig. 8. Geometry and source power information of the problem: (a) Solid layer with three circular cylindrical inclusions, bounded by two unbounded fluid media; (b) Heating curve of the source.

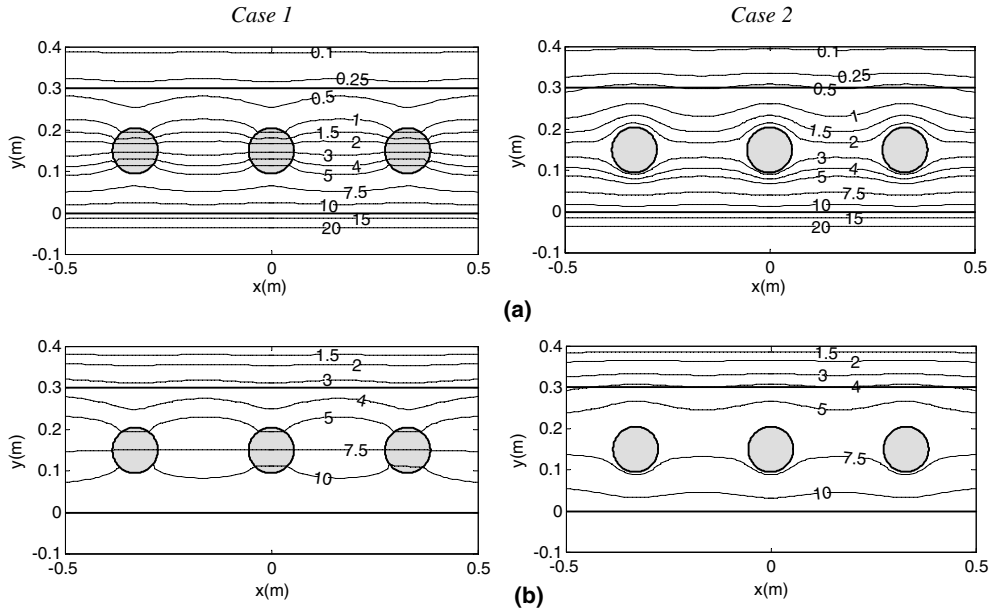

Fig. 9. Distribution of temperature registered at a grid of receivers for a homogeneous concrete layer with circular inclusions of polystyrene (Case1) and steel (Case2), when convection velocity is ascribed to the top and bottom media: (a) $t = 10$ h; (b) $t = 20$ h.

unbounded media were kept constant and similar to those of the water: $k = 0.606\ \mathrm{W\,m^{-1}\,^{\circ}C^{-1}}$, $c = 4181\ \mathrm{J\,kg^{-1}\,^{\circ}C^{-1}}$ and $\rho = 998.0\ \mathrm{kg\,m^{-3}}$.

The calculations are first performed in the frequency domain [0, $128 \times 0.5 \times 10^{-5}$ Hz], with a frequency increment of 0.5×10^{-5} Hz. This defines a time window with a total duration of 55.56 h. Null initial temperatures and heat fluxes are prescribed along the full domain.

These systems were subjected to a plane heat source placed in the lower medium ($y_0 = -0.1$ m). The energy emitted by the plane heat source was assumed to have a trapezoidal evolution, as shown in Fig. 8b. The heat source starts emitting energy at $t \approx 0.76$ h and its power is increased linearly from 0.0 W to 1000.0 W, reaching maximum power at $t \approx 3.46$ h; the source keeps introducing heat into the system, continuously, for a period of $t \approx 2.72$ h; the power then falls linearly; it reaches 0.0 W at $t \approx 8.89$ h. Note that different temporal power source evolutions could be easily implemented.

Fig. 9 presents contour plots obtained at $t = 10$ h and $t = 20$ h, using the temperature amplitudes obtained over a fine grid of receivers. The convection phenomenon is modelled assuming that its origin coincides with the position of the heat source. The marked differences observed between the computations performed for Case 1 and Case 2 scenarios are attributed to the different thermal properties of the inclusions, since the rest of system remains the same. The temperature curves in the presence of the polystyrene inclusions (Case 1) reveal higher temperatures at the bottom of the inclusions and lower temperatures behind the inclusion when compared with the Case 2 (steel inclusions). The energy being accumulated at the source side of the inclusions, observed in the Case 1, is due to the low thermal diffusivity coefficient of the polystyrene.

For comparison, Fig. 10 displays similar results computed when no convection is allowed in the fluid media. Comparing the two cases in Figs. 9 and 10 at $t = 10$ h, it is interesting to note that the heat spreads faster when positive vertical convection velocities are ascribed to the top and bottom media. Higher temperatures are therefore registered along the solid media. At $t = 20$ h, the heating sources are already switched off. However, as can be seen for both cases analysed, the energy is still propagating across the domain, since the heat equilibrium is not completed.

To better illustrate the time evolution of the heat diffusion, the results computed at three receivers are shown in Fig. 11. The receivers Rec. 1, Rec. 2 and Rec. 3 are placed at ($x = 0.0$ m, $y = 0.073$ m), ($x = 0.0$ m, $y = 0.145$ m) and ($x = 0.0$ m, $y = 0.216$ m), respectively, as displayed in Fig. 8a.

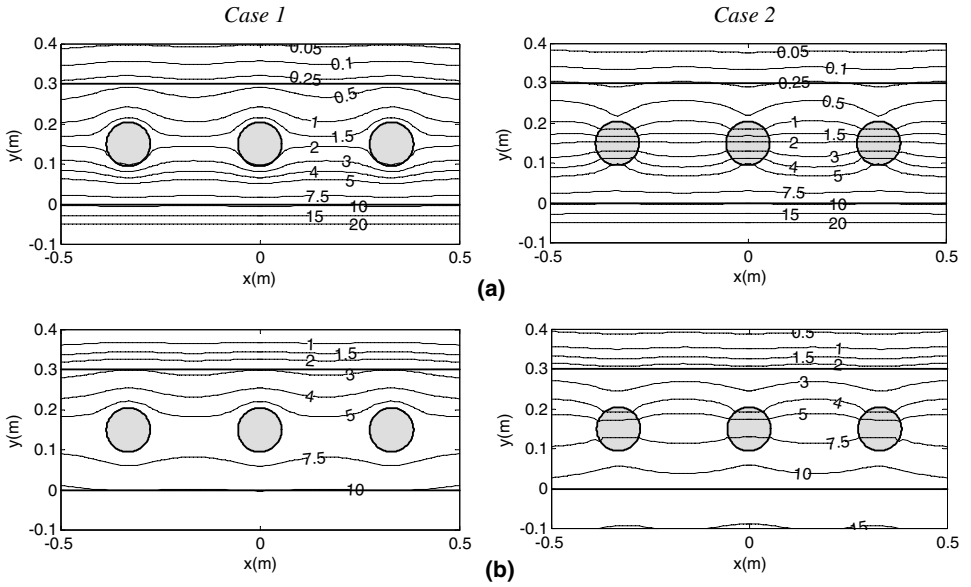

Fig. 10. Distribution of temperature registered at a grid of receivers for a homogeneous concrete layer with circular inclusions of polystyrene (Case1) and steel (Case2), considering only the conduction phenomenon: (a) $t = 10$ h; (b) $t = 20$ h.

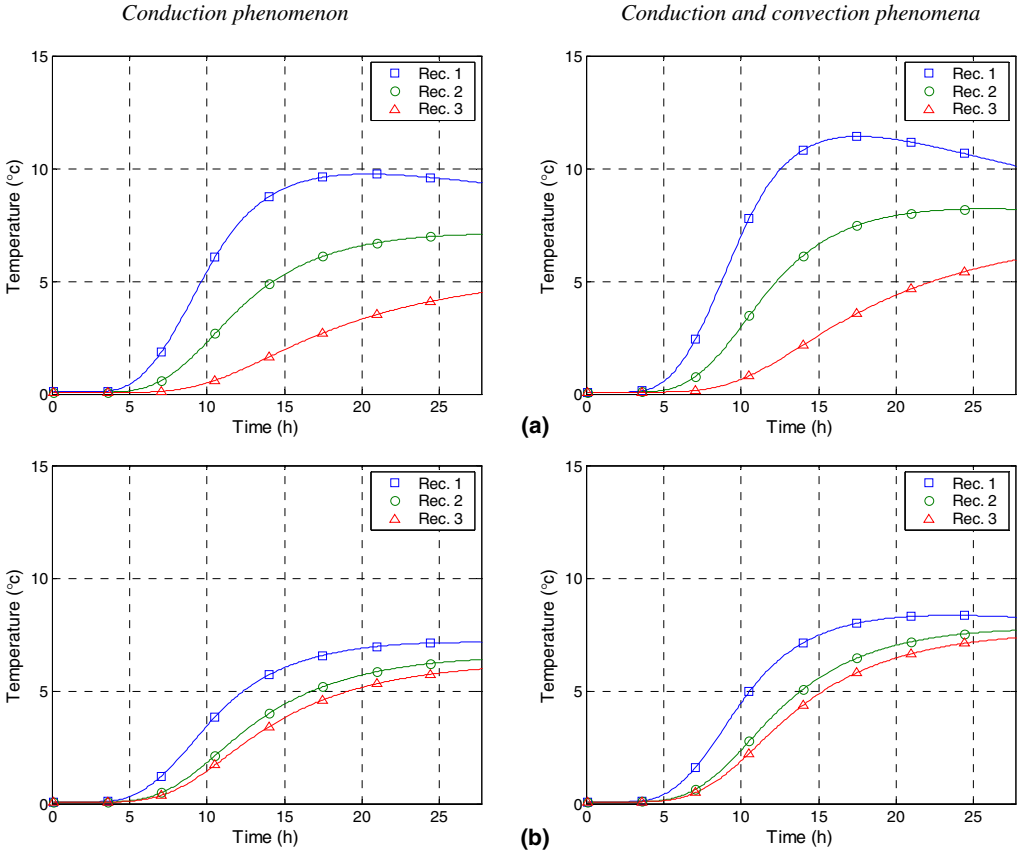

Fig. 11. Temperature evolution at the receivers Rec. 1, 2 and 3: (a) Case 1 (polystyrene inclusions); (b) Case 2 (steel inclusions).

The receiver Rec.1, which is closer to the position of the heat plane source, is the first to record a progressive change of temperature. The higher temperatures registered at the Rec. 1 when the inclusion is made of polystyrene (Case 1) confirm its insulating properties. The receiver placed inside the polystyrene inclusion also records higher temperatures than those registered in the steel inclusion, because the energy does not propagate easily through this material. Notice also that, the receiver located immediately behind the inclusion (receiver 3) registers lower temperatures when the inclusion is made of polystyrene (Case 1).

The results illustrated in Fig. 11 show that, in the time window being studied, only the receiver nearest the heat source records a fall in temperature after the source power has dropped to 0 W. In fact, the temperature is still increasing at the receivers placed further away from the heat source. The energy equilibrium along the domain takes a long time to be established, as can be predicted from the results obtained for a time window of 25.55 h.

The modelling of the positive convection velocity along the y direction introduces marked differences in the thermal response along the domain. For example the receiver Rec. 1 registers a maximum temperature of 11.4 °C when both conduction and convection phenomena are modelled, while the same receiver in the presence of the conduction alone records a temperature of 9.75 °C. The presence of the convection enables the heat to flow faster, and so the temperature falls sooner.

Once the source has reached the maximum power, the differences between the temperatures registered at the receivers is seen to be higher in the presence of the extruded polystyrene inclusions (Case 1). The opposite behaviour (small thermal gradient) is found in Case 2 because the steel allows higher thermal diffusivity. The temperature variation inside the steel inclusion is very small; as a consequence, the temperature curve for Rec. 2 and 3 are very close and similar (see Fig. 11b).

Finally, it is important to remember that the heat transfer across a layer formation can be affected to a considerable extent by the presence of thermal heterogeneities and the convection phenomenon. The proposed formulation can help to model this kind of problem with greater efficiency.

7. Conclusions

The transient heat transfer by conduction and convection across a solid layer with heterogeneities, bounded by two semi-infinite media has been described.

This paper has illustrated how heat diffusion can be determined in the frequency domain, reformulating the mathematical and numerical formulations found in other fields such as wave problems. The BEM technique proposed can handle any type of heat source and allows the modelling of layered media without having to discretize the solid interfaces. A series of verifications were performed to assure the formulation's accuracy: the verification of the frequency domain approach using the Green's functions for the unbounded medium; the verification of the Green's functions for a layered formation; and the verification of the formulation based on a BEM model that includes the Green's functions for the layered formation.

The proposed formulation was used to compute the temperature distribution evolution for a solid layer containing several thermal heterogeneities. Different thermal properties were prescribed for the inclusions and both the conduction and convection phenomena were modelled. The results obtained demonstrate the particular importance of the convection phenomenon, and the marked influence of the thermal heterogeneities on the heat transfer across a layered formation.

References

[1] C.A. Brebbia, J.C.F. Telles, L.C. Wrobel, Boundary Element Techniques: Theory and Applications in Engineering, Springer, Berlin, 1984.
[2] M.L.G. Pina, J.L.M. Fernandez, Applications in heat conduction by BEM, in: C.A. Brebbia (Ed.), Topics in Boundary Element Research, Springer, Berlin, 1984.
[3] Y.P. Chang, C.S. Kang, D.J. Chen, The use of fundamental Green's functions for solution of problems of heat conduction in anisotropic media, Int. J. Heat Mass Transfer 16 (1973) 1905–1918.
[4] R.P. Shaw, An integral equation approach to diffusion, Int. J. Heat Mass Transfer 17 (1974) 693–699.
[5] L.C. Wrobel, C.A. Brebbia, A formulation of the boundary element method for axisymmetric transient heat conduction, Int. J. Heat Mass Transfer 24 (1981) 843–850.

[6] A. Carini, M. Diligenti, A. Salvadori, Implementation of a symmetric boundary element method in transient heat conduction with semi-analytical integrations, Int. J. Numer. Methods Eng. 46 (1999) 1819–1843.
[7] D. Lesnic, L. Elliot, D.B. Ingham, Treatment of singularities in time-dependent problems using the boundary element method, Eng. Anal. Bound. Elem. EABE 16 (1995) 65–70.
[8] A. Sutradhar, G.H. Paulino, L.J. Gray, Transient heat conduction in homogeneous and non-homogeneous materials by the Laplace transform Galerkin boundary element method, Eng. Anal. Bound. Elem. EABE 26 (2) (2002) 119–132.
[9] A. Sutradhar, G.H. Paulino, The simple boundary element method for transient heat conduction in functionally graded materials, Comput. Methods Appl. Mech. Eng. 193 (2004) 4511–4539.
[10] D. Nardini, C.A. Brebbia, A new approach to free vibration analysis using boundary elements, Boundary Element Methods in Engineering, Computational Mechanics Publications/Springer-Verlag, Southampton/Berlin, 1982.
[11] S.P. Zhu, P. Satravaha, An efficient computational method for nonlinear transient heat conduction problems, Appl. Math. Model. 20 (1996) 513–522.
[12] P. Satravaha, S. Zhu, An application of the LTDRM to transient diffusion problems with nonlinear material properties and nonlinear boundary conditions, Appl. Math. Comput. 87 (1997) 127–160.
[13] I. Guven, E. Madenci, Transient heat conduction analysis in a piecewise homogeneous domain by a coupled boundary and finite element method, Int. J. Numer. Methods. Eng. 56 (2003) 351–380.
[14] M. Tanaka, K. Tanaka, Transient heat conduction problems in inhomogeneous media discretized by means of boundary volume element, Nucl. Eng. Des. 60 (1980) 381–387.
[15] R. Butterfield, An application of the boundary element method to potential flow problems in generally inhomogeneous bodies, in: C.A. Brebbia (Ed.), Recent Advances in Boundary Element Method, Pentech Press, London, 1978.
[16] J. Sladek, V. Sladek, Ch. Zhang, A local BIEM for analysis of transient heat conduction with nonlinear source terms in FGMs, Eng. Anal. Bound. Elem. EABE 28 (2004) 1–11.
[17] A. Tadeu, J. António, L. Godinho, N. Simões, Boundary element method analyses of transient heat conduction in an unbounded solid layer containing inclusions, Comput. Mech. 34 (2004) 99–110.
[18] H. Lamb, On the propagation of tremors at the surface of an elastic solid, Philos. Trans. Roy. Soc. London A203 (1904) 1–42.
[19] M. Bouchon, Discrete wave number representation of elastic wave fields in three-space dimensions, J. Geophys. Res. 84 (1979) 3609–3614.
[20] A. Tadeu, J. António, 2.5D Green's functions for elastodynamic problems in layered acoustic and elastic formations, J. Comput. Model. Eng. Sci. CMES 2 (4) (2001) 477–495.
[21] P.K. Banerjee, The Boundary Element Methods in Engineering, McGraw-Hill, England, 1981.
[22] H.S. Carslaw, J.C. Jaeger, Conduction of Heat in Solids, second ed., Oxford University Press, 1959.
[23] Gradshteyn, Ryzhik, Tables of integrals, series, and products, 1980.
[24] L. Schwartz, Theorie des distributions, Hermann, Paris, 1966.
[25] M. Bouchon, K. Aki, Time-domain transient elastodynamic analysis of 3D solids by BEM, Int. J. Numer. Methods Eng. 26 (1977) 1709–1728.
[26] A. Tadeu, L. Godinho, P. Santos, Wave motion between two fluid filled boreholes in an elastic medium, Eng. Anal. Bound. Elem. EABE 26 (2) (2002) 101–117.
[27] L. Godinho, J. António, A. Tadeu, 3D sound scattering by rigid barriers in the vicinity of tall buildings, J. Appl. Acoust. 62 (11) (2001) 1229–1248.
[28] W. Garvin, Exact transient solution of the buried line source problem, Proc. Roy. Soc. London, Ser. A – Math. Phys. Sci. 234 (1199) (1955) 528–541.
[29] P.M. Morse, Feshbach Methods of Theoretical Physics, McGraw-Hill, New York, 1953, p. 823.
[30] E. Kausel, J.M. Roësset, Frequency domain analysis of undamped systems, J. Eng. Mech. ASCE 118 (4) (1992) 721–734.
[31] A. Tadeu, P. Santos, E. Kausel, Closed-form integration of singular terms for constant, linear and quadratic boundary elements – Part I: SH wave propagation, Eng. Anal. Bound. Elem. EABE 23 (8) (1999) 671–681.
[32] A. Tadeu, P. Santos, E. Kausel, Closed-form integration of singular terms for constant, linear and quadratic boundary elements – Part II: SV-P wave propagation, Eng. Anal. Bound. Elem. EABE 23 (9) (1999) 757–768.
[33] R.A. Phinney, Theoretical calculation of the spectrum of first arrivals in the layered elastic medium, J. Geophys. Res. 70 (1965) 5107–5123.